

Propensities for the formation of individual disulfide bonds in hen lysozyme and the size and stability of disulfide-associated submolecular structures

Hideki Tachibana*

Department of Biology, Faculty of Science, and Graduate School of Science and Technology, Kobe University, Rokkodai, Nada-ku, Kobe 657-8501, Japan

Received 5 July 2000; accepted 19 July 2000

Edited by Thomas L. James

Abstract Hen lysozyme single-disulfide variants were constructed to characterize the structures associated with the formation of individual native disulfide bonds. Circular dichroism spectra and the effective concentration of protein thiol groups showed that the propensity for structure formation was relatively high for Cys-6–Cys-127 and Cys-30–Cys-115 disulfides. The urea concentration dependence of individual effective concentrations showed that the apparent sizes of the structures were 14–50% of the whole molecule. The intrinsic stability of each submolecular structure in a reduced form of protein, obtained by subtracting the entropic contribution of cross-linking, was highest for Cys-64–Cys-80 and lowest for Cys-76–Cys-94 disulfide bonds. © 2000 Federation of European Biochemical Societies. Published by Elsevier Science B.V. All rights reserved.

Key words: Hen lysozyme; Disulfide bond; Effective concentration; Oxidative folding

1. Introduction

The formation of disulfide bonds in a protein is generally coupled with the formation of higher order structures. Certain proteins attain completely folded and global structures in the reduced form [1–3]. The folding reaction is cooperative over the entire polypeptide chain, and disulfide bonds add extra thermodynamic stability. Other proteins do not have substantial structures in a reduced form as well as in disulfide-intermediates. Here, in one case, if the cooperativity is high, the protein structure may be globally formed, but the population of the folded state is low; in the other case, the cooperativity is low, and each disulfide-bond formation is associated with the formation of local structures [4–7].

Hen lysozyme contains four disulfide bonds. Its four three-disulfide (3SS) derivatives all have secondary and tertiary structures as well as enzymatic activity comparable to those

of authentic lysozyme, and show cooperative unfolding transitions [8–10]. On the other hand, its reduced form retains only a residual amount of secondary structure, and lacks tertiary structure and enzymatic activity [11,12]. We have constructed here four species of hen lysozyme 1SS variants (Fig. 1), and characterized the structures that are associated with the formation of individual native disulfide bonds with circular dichroism (CD) spectroscopy and the measurement of the effective concentration (C_{eff}) of protein thiol groups [13]. The urea concentration dependence of individual C_{eff} s was analyzed to obtain submolecular size and intrinsic stability of the structures.

2. Materials and methods

2.1. Hen lysozyme single-disulfide variants

Each gene for the 1SS variants was constructed by recombining one of the 3SS variant genes [8,9] with one of the 2SS variant genes synthesized for the present study, at two restriction sites (*Csp45I* and *MluI*) within a coding region. For instance, the gene for 1SS-3 was constructed by the ligation of the 3SS- Δ 4Ala-derived fragment that covers amino acid residues 31–107 and contains the replacements Cys-76→Ala and Cys-94→Ala with the 2SS- Δ (1+2)-derived fragment that covers amino acid residues 1–30 as well as 108–129 (and a vector region) and contains the replacement Cys-6→Ser, Cys-30→Ala, Cys-115→Ala and Cys-127→Ala, resulting in a gene that retains Cys residues 64 and 80. The gene for a 0SS variant, which retains no cysteinyl residues, was constructed by recombining the 2SS- Δ (1+2) gene with the 2SS- Δ (3+4) gene. The nucleotide sequences were confirmed by dideoxy sequencing. The expression of the genes and purification of polypeptides were carried out as described [9]. The N-terminal methionine residue is attached unexcised in each variant.

2.2. CD spectroscopy

Several mg of the reduced 1SS variant was air-oxidized in 100 mM Tris-acetate, 2 μ M CuCl₂, pH 7.85, at 25°C for 15 h at the protein concentration of 3.3 μ M; concentrated with ultrafiltration; and purified with reverse-phase HPLC on a Waters μ Bondasphere C4 column (19×150 mm). CD spectra were taken in 20 mM sodium acetate, pH 4.0, by using a J-720 spectropolarimeter (Japan Spectroscopic Co.). Far-UV thermal unfolding curves were obtained by using a Peltier-type temperature controller.

2.3. Effective concentration measurements

The equilibrium disulfide formation reaction was carried out in 100 mM Tris-acetate, 0.1 mM EDTA, pH 7.85, in the presence of 0.1 mM oxidized glutathione (GSSG) and 1 mM reduced glutathione (GSH) with a protein concentration of 3.3 μ M. The solution conditions with no denaturant are called 'native solution conditions'. GuHCl or urea (biochemical grade, Wako Pure Chemical Industries, Ltd.) was included when indicated, and the solution conditions containing 6 M GuHCl are called 'denaturing solution conditions'. The reaction was stopped by adding acetic acid to 1 M, and the product was subjected to reverse-phase HPLC on Waters μ Bondasphere C4

*Fax: (81)-78-803 5711.

E-mail: tachiban@biol.kobe-u.ac.jp

Abbreviations: C_{eff} , effective concentration; C_{eff}^D , effective concentration under denaturing solution conditions; GSH, reduced glutathione; GSSG, oxidized glutathione; Oxi, oxidized form of protein; Red, reduced form of protein; SS*n* (*n*=1–4), each of the four native disulfide bonds in hen lysozyme between Cys residues 6–127, 30–115, 64–80, and 76–94, for *n*=1, 2, 3, and 4, respectively; 1SS-*n* (*n*=1–4), single-disulfide variant of hen lysozyme that retains SS*n*; 3SS, three-disulfide

columns (two columns, each 3.9×150 mm, connected in tandem) at 40°C , in 0.05% TFA with a gradient of acetonitrile from 32.0 to 36.0% in 50 min. C_{eff} was calculated from the peak areas for the reduced (Red) and oxidized (Oxi) form of the protein as described [14,15]: $C_{\text{eff}} = [\text{Oxi}][\text{GSH}]^2/[\text{Red}][\text{GSSG}]$.

3. Results and discussion

3.1. Overall structure and stability of the oxidized form of ISS variants

The amount of secondary structure in the reduced form of hen lysozyme is significantly lower than that of authentic lysozyme [12,16]. This was equally true for the OSS variant, whose far-UV CD spectrum (Fig. 2A) was nearly identical to the spectrum reported for the reduced form [16]. The increase in secondary structure accompanying the formation of each single disulfide bond, i.e. in excess of that of the OSS variant, was less than half as much as that observed for authentic lysozyme, and relatively large for ISS-1 and ISS-2 in this order, while not significant in ISS-3 or ISS-4. No ISS variants showed near-UV CD bands or bacteriolytic activity, indicating that an all-or-nothing type, globally cooperative structure formation did not occur. The highly gradual thermal unfolding curves (Fig. 2B) showed that the locally folded states were not stable even at low temperatures at pH 4. Urea-unfolding curves for these ISS variants monitored with optical spectroscopy were also too diffuse to permit reliable quantitative analyses.

3.2. Effective concentration of cysteinyl thiol groups participating in each disulfide bond

To probe such local structures in sensitive and specific ways, the C_{eff} of cysteinyl thiol groups in each variant was measured (Fig. 3 and Table 1). It was highest for SS3, substantially lower for SS4, and a little lower for SS2 and SS1. The result is in accordance with the previous observation that the two disulfides involving Cys-64, Cys-76, Cys-80, and Cys-94 form faster than those involving Cys-6, Cys-30, Cys-115, and Cys-127 do [17]. As expected, the C_{eff} under denaturing solution conditions ($C_{\text{eff}}^{\text{D}}$) was smaller for disulfide bonds that form larger polypeptide loops. According to a regression analysis, $C_{\text{eff}}^{\text{D}}$ values depended on the loop size with an exponent

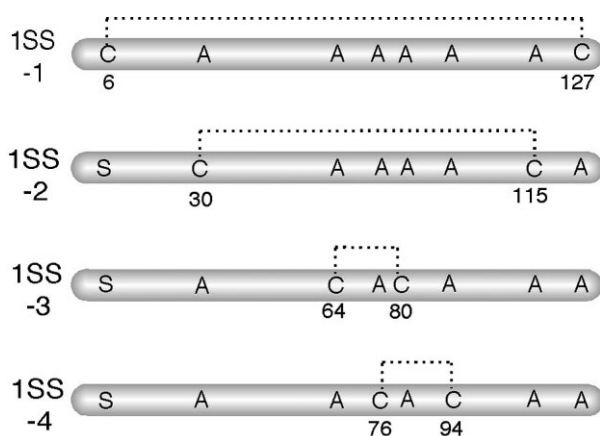


Fig. 1. Primary structure of the four ISS variants. C, A, and S denote cysteinyl, alanyl, and seryl residues, respectively. The numbers beneath them denote the residue positions.

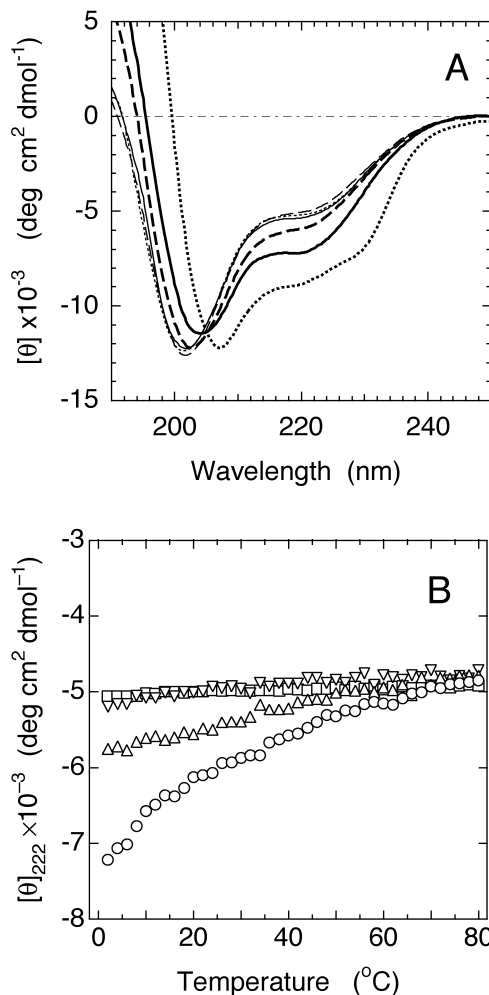


Fig. 2. A: Far-UV CD spectra of the oxidized form of ISS variants measured at 4°C : ISS-1 (thick full line), ISS-2 (thick broken line), ISS-3 (thin full line), and ISS-4 (thin broken line). The spectra for authentic lysozyme (thick dotted line) and the OSS variant (thin dotted line) are also shown. B: Thermal unfolding of the oxidized form of ISS variants at pH 4.0: ISS-1 (circle), ISS-2 (up triangle), ISS-3 (down triangle), and ISS-4 (square).

of -1.59 ± 0.11 , close to the value -1.5 expected for a random coil chain.

Remarkably, the C_{eff} values for SS1 and SS2 showed a large relative increase accompanying the change from denaturing to native solution conditions. This is in accordance with the relatively large amount of secondary structure observed for them. In authentic lysozyme, SS1 and SS2 are contained in the α -domain, which contains a hydrophobic core. Peptide fragments that constitute this domain have high propensity for structure formation [18,19]. However, the C_{eff} for SS2 is not so high as the corresponding disulfide bond Cys-28–Cys-111 of human α -lactalbumin (1070 mM [20]), which is closely homologous with lysozyme [21]. This appears to be related with the considerably high propensity for secondary structure formation in α -lactalbumin [20,22,23]. The ratio $C_{\text{eff}}^{\text{D}}/C_{\text{eff}}$ was much lower for SS3 and SS4.

3.3. Urea concentration dependence of C_{eff} and apparent size of the protein submolecular structure associated with each disulfide bond formation

The dependence of C_{eff} on [urea] is shown in Fig. 4. At 8 M

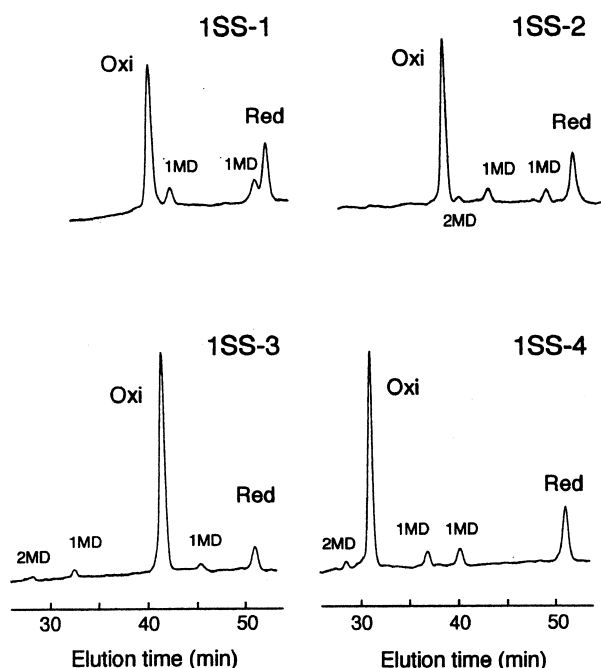
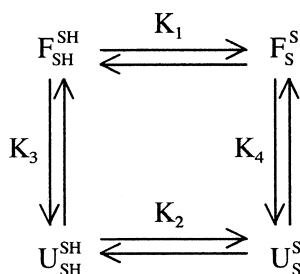


Fig. 3. The Oxi and Red forms of each ISS variant, equilibrated at 25°C for 4 h under native solution conditions, were separated with reverse-phase HPLC. The labels 1MD and 2MD indicate single-mixed-disulfide and double-mixed-disulfide species, respectively. The 2MD for 1SS-1 elutes just after, and partially overlaps with, the Oxi-peak.

urea, the C_{eff} s for individual disulfide bonds were nearly equal, respectively, to those obtained at 6 M GuHCl. With decreasing urea concentrations C_{eff} values increased, but did not reach saturation at 0 M urea, indicating that the folded states are not populated 100%. Thus, the C_{eff} values under native solution conditions do not represent those for completely folded states. Assuming that individual disulfide-associated local folding reactions occur in two-state mechanisms, we exploit the linkage relationship between reduction–oxidation and unfolding–folding equilibria:



Here, folded–reduced ($F_{\text{SH}}^{\text{SH}}$), folded–oxidized (F_{S}^{S}), unfolded–reduced ($U_{\text{SH}}^{\text{SH}}$), and unfolded–oxidized (U_{S}^{S}) states are considered. K_1 and K_2 represent the pseudo equilibrium constants for the half reactions of disulfide formation in the 100% folded and 100% unfolded states, respectively [14]. K_3 and K_4 represent the equilibrium constants for the unfolding reaction of reduced and oxidized proteins, respectively.

When F- and U-states coexist with each other,

$$C_{\text{eff}} = C_{\text{eff}}^{\text{F}} (1/(1 + K_3)) + C_{\text{eff}}^{\text{U}} (K_3/(1 + K_3)) \quad (1)$$

where $C_{\text{eff}}^{\text{F}} = K_1/([GSSG]/[GSH]^2)$ and $C_{\text{eff}}^{\text{U}} = K_2/([GSSG]/$

$[GSH]^2)$ [24]. In the present case, $C_{\text{eff}}^{\text{U}}$ can be equated with the $C_{\text{eff}}^{\text{D}}$ described above. However, $C_{\text{eff}}^{\text{F}}$ cannot be determined experimentally, leaving K_3 undetermined. If a reduced–folded state is highly unstable under native solution conditions, i.e. $K_3 \gg 1$, and if we substitute $\exp(-(\Delta G_o - m[\text{urea}])/RT)$ for K_3 as in conventional treatment of urea-unfolding curves [25], then:

$$C_{\text{eff}} \approx C_{\text{eff}}^{\text{F}}/K_3 + C_{\text{eff}}^{\text{D}} = C_{\text{eff}}^{\text{F}} \exp(\Delta G_o/RT)$$

$$\times \exp(-m[\text{urea}]/RT) + C_{\text{eff}}^{\text{D}} \quad (2)$$

Here, ΔG_o refers to the intrinsic stability in a reduced form (and therefore free from the entropic stabilizing effect by a disulfide cross-link) of a submolecular structure that will be coupled with the formation of a disulfide bond under oxidizing conditions; and m represents the amount of differential interaction of protein submolecular structure between its folded and unfolded states with the denaturant, and is a rough measure of cooperativity or the size of submolecular structure. The C_{eff} versus [urea] data were regressed to Eq. 2, and obtained m values were shown in Table 1.

The apparent size of the structure is largest for SS1, smallest for SS3, and considerably smaller than that for the urea-unfolding of disulfide-intact authentic lysozyme [26,27]. In authentic lysozyme, SS1 and SS2 link the regions that are rich in secondary structures, while SS3 links regions that are poor [28], suggesting that the size may correlate with the amount of secondary structures that can occur at or near the two participating Cys residues. An m value similar to that for SS3 has been reported for the disulfide bond Cys-14–Cys-38 of bovine pancreatic trypsin inhibitor [29].

3.4. Estimation of the intrinsic stability of submolecular structures in a reduced form

$C_{\text{eff}}^{\text{F}}$ and ΔG_o could not be independently determined above. They could be estimated, however, as follows. The thermodynamic linkage relationship $K_1 \times K_4 = K_3 \times K_2$ leads into $C_{\text{eff}}^{\text{F}}/C_{\text{eff}}^{\text{U}} = K_1/K_2 = K_3/K_4 = \exp(-\Delta\Delta G/RT)$, where $\Delta\Delta G$ is a difference, between reduced and oxidized forms of protein, in the free energy change for the unfolding of protein struc-

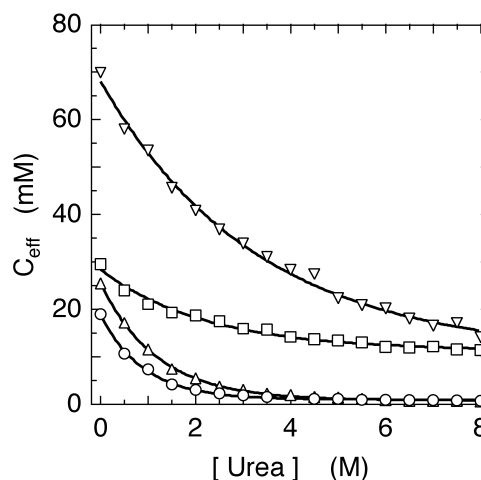


Fig. 4. Urea-concentration dependence of the C_{eff} for each of the four disulfide bonds, measured at 25°C: SS1 (circle), SS2 (up triangle), SS3 (down triangle), and SS4 (square).

Table 1

Propensities for individual disulfide bond formation and thermodynamic parameters for the submolecular structures associated with individual disulfide bonds

	Loop size	C_{eff} (mM) ^a	$C_{\text{eff}}^{\text{D}}$ (mM) ^a	$C_{\text{eff}}/C_{\text{eff}}^{\text{D}}$	m (kJ mol ⁻¹ M ⁻¹) (m/m_w , %) ^b	δS (J mol ⁻¹ K ⁻¹)	$\exp(\delta S/R)$	ΔG_o (kJ mol ⁻¹)
SS1	121	21 ± 2	0.66 ± 0.12	32 ± 9	2.72 ± 0.80 (50)	88.7	42 800	-17.9 ± 0.9
SS2	85	26 ± 4	0.81 ± 0.07	32 ± 8	2.10 ± 0.29 (39)	84.3	25 200	-16.6 ± 0.8
SS3	16	72 ± 6	13.2 ± 1.2	5.5 ± 0.9	0.75 ± 0.25 (14)	63.5	2 060	-15.2 ± 0.6
SS4	18	29 ± 3	12.8 ± 1.2	2.3 ± 0.5	1.09 ± 0.13 (20)	64.9	2 460	-18.7 ± 1.2

^aValues obtained at 25°C. Mean ± S.D. for three to six measurements were shown.

^bRatio of m to that for the whole molecule, m_w (= 5.41 kJ mol⁻¹ M⁻¹ [27]).

ture [14]. We assume that $\Delta\Delta G$ stems solely from the difference in the conformational entropy (δS) of unfolded polypeptide chain between reduced and oxidized forms. Then, $C_{\text{eff}}^{\text{F}}/C_{\text{eff}}^{\text{U}} = \exp(\delta S/R)$. The δS estimated by using equation: $R \times (3.47 + 1.5 \times \ln(\text{loop size}))$ [30] and $\exp(\delta S/R)$ for each disulfide bond are shown in Table 1. When $C_{\text{eff}}^{\text{F}}/C_{\text{eff}}^{\text{U}} = C_{\text{eff}}^{\text{F}}/C_{\text{eff}}^{\text{D}} = \exp(\delta S/R) \gg 1$ and [urea] = 0, Eq. 2 reduces to:

$$\ln(C_{\text{eff}}/C_{\text{eff}}^{\text{D}} - 1) \approx \ln(C_{\text{eff}}^{\text{F}}/C_{\text{eff}}^{\text{D}}) + \Delta G_o/RT$$

$$= \delta S/R + \Delta G_o/RT \quad (3)$$

Using the experimentally obtained $C_{\text{eff}}/C_{\text{eff}}^{\text{D}}$ (Table 1) and theoretically calculated δS , we estimated ΔG_o (Table 1).

The negative ΔG_o values indicate the predominance of the unfolded states in a reduced form. The intrinsic stability of the SS1-associated submolecular structure is not particularly high. Thus, the highest amount of secondary structure and the largest value of m for SS1 are primarily due to a high entropic contribution of cross-linking, which is highest for SS1 since the loop size is largest. The SS3-associated structure is intrinsically least unstable and the SS4-associated one most unstable. Overall, the intrinsic stability of submolecular structure is relatively high for SS3 and SS2. These conclusions were not altered when a different parameter value [3] was used in the estimation of δS . We note that the 2SS derivative obtained as the only intermediate during reduction of authentic lysozyme retains SS2 and SS3 [31].

In summary, we have shown that in 0SS-to-1SS stage of oxidative folding of hen lysozyme the formation of individual disulfide bonds is coupled with the formation of submolecular structures of different size and intrinsic stability to result in different overall propensities.

Acknowledgements: The author thanks Dr. K. Akasaka and Dr. S. Segawa for valuable discussions and the facilities of CD measurements, Mr. H. Sawano for constructing variant genes, and Mr. T. Ohta for thermal unfolding measurements. This work was partly supported by grants-in-aid for scientific research from the Ministry of Education, Science and Culture, Japan.

References

- [1] Goto, Y. and Hamaguchi, K. (1979) *J. Biochem.* 86, 1433–1441.
- [2] Oobatake, M., Takahashi, S. and Ooi, T. (1979) *J. Biochem.* 86, 65–70.
- [3] Pace, C.N., Grimsley, G.R., Thomson, J.A. and Barnett, B.J. (1988) *J. Biol. Chem.* 263, 11820–11825.
- [4] van Mierlo, C.P.M., Darby, N.J. and Creighton, T.E. (1992) *Proc. Natl. Acad. Sci. USA* 89, 6775–6779.
- [5] van Mierlo, C.P.M., Darby, N.J., Keeler, J., Neuhaus, D. and Creighton, T.E. (1993) *J. Mol. Biol.* 299, 1125–1146.
- [6] Ewbank, J.J. and Creighton, T.E. (1993) *Biochemistry* 32, 3694–3707.
- [7] Wu, L.C., Peng, Z. and Kim, P.S. (1995) *Nature Struct. Biol.* 2, 281–286.
- [8] Sawano, H., Koumoto, Y., Ohta, K., Sasaki, Y., Segawa, S. and Tachibana, H. (1992) *FEBS Lett.* 303, 11–14.
- [9] Tachibana, H., Ohta, Y., Sawano, H., Koumoto, Y. and Segawa, S. (1994) *Biochemistry* 33, 15008–15016.
- [10] Yokota, A., Izutani, K., Takai, M., Kubo, Y., Noda, Y., Koumoto, Y., Tachibana, H. and Segawa, S. (2000) *J. Mol. Biol.* 295, 1275–1288.
- [11] Yutani, K., Yutani, A., Imanishi, T. and Isemura, T. (1968) *J. Biochem.* 64, 449–455.
- [12] Saxena, V.P. and Wetlaufer, D.B. (1970) *Biochemistry* 9, 5015–5023.
- [13] Creighton, T.E. (1983) *Biopolymers* 22, 49–58.
- [14] Lin, T.-Y. and Kim, P.S. (1989) *Biochemistry* 28, 5282–5287.
- [15] Darby, N.J. and Creighton, T.E. (1993) *J. Mol. Biol.* 232, 873–896.
- [16] White Jr., F.H. (1976) *Biochemistry* 15, 2906–2912.
- [17] Anderson, W.L. and Wetlaufer, D.B. (1976) *J. Biol. Chem.* 251, 3147–3153.
- [18] Segawa, S., Fukuno, T., Fujiwara, K. and Noda, Y. (1991) *Biopolymers* 31, 497–509.
- [19] Yang, J.J., Buck, M., Pitkeathly, M., Kotik, M., Haynie, D.T., Dobson, C.M. and Radford, S.E. (1995) *J. Mol. Biol.* 252, 483–491.
- [20] Peng, Z.-Y., Wu, L.C. and Kim, P.S. (1995) *Biochemistry* 34, 3248–3252.
- [21] McKenzie, H.A. (1996) in: *Lysozymes: Model Enzymes in Biochemistry and Biology* (Jollès, P., Ed.), pp. 365–409, Birkhäuser Verlag, Basel.
- [22] Lewis, P.N. and Scheraga, H.A. (1971) *Arch. Biochem. Biophys.* 144, 584–588.
- [23] Redfield, C., Schulman, B.A., Milhollen, M.A., Kim, P.S. and Dobson, C.M. (1999) *Nature Struct. Biol.* 6, 948–952.
- [24] Lin, T.-Y. and Kim, P.S. (1991) *Proc. Natl. Acad. Sci. USA* 88, 10573–10577.
- [25] Pace, C.N. (1986) *Methods Enzymol.* 131, 266–280.
- [26] Greene Jr., R.R. and Pace, C.N. (1974) *J. Biol. Chem.* 249, 5388–5393.
- [27] Ahmad, F. and Bigelow, C.C. (1982) *J. Biol. Chem.* 257, 12935–12938.
- [28] Blake, C.C.F., Koenig, D.F., Mair, G.A., North, A.C.T., Phillips, D.C. and Sarma, V.R. (1965) *Nature* 206, 757–761.
- [29] Zdanowski, K. and Dadlez, M. (1999) *J. Mol. Biol.* 287, 433–445.
- [30] Lin, S.H., Konishi, Y., Denton, M.E. and Scheraga, H. (1984) *Biochemistry* 23, 5504–5512.
- [31] Acharya, A.S. and Taniuchi, H. (1980) *Int. J. Pept. Protein Res.* 15, 503–509.